emeraldinsight

Industrial Robot: An International Journal

Mechanical design and error prediction of a flexible manipulator system applied in nuclear fusion environment

Shanshuang Shi, Huapeng Wu, Yuntao Song, Heikki Handroos,

Article information:

To cite this document:
Shanshuang Shi, Huapeng Wu, Yuntao Song, Heikki Handroos, (2017) "Mechanical design and error prediction of a flexible manipulator system applied in nuclear fusion environment", Industrial Robot: An International Journal, Vol. 44 Issue: 6, pp.711-719, https://doi.org/10.1108/IR-04-2017-0066
Permanent link to this document:
https://doi.org/10.1108/IR-04-2017-0066

Downloaded on: 21 January 2018, At: 18:57 (PT)
References: this document contains references to 19 other documents.
To copy this document: permissions@emeraldinsight.com
The fulltext of this document has been downloaded 58 times since 2017*

Users who downloaded this article also downloaded:

(2017),"Human robot interaction for manipulation tasks based on stroke gesture recognition", Industrial Robot: An International Journal, Vol. 44 Iss 6 pp. 700-710 https://doi.org/10.1108/IR-01-2017-0011

(2017),"Integration of fault tree analysis, reliability block diagram and hazard decision tree for industrial robot reliability evaluation", Industrial Robot: An International Journal, Vol. 44 Iss 6 pp. 754-764 https://doi.org/10.1108/IR-06-2017-0103

The University of Nottingham

Access to this document was granted through an Emerald subscription provided by emerald-srm:311681 []

For Authors

If you would like to write for this, or any other Emerald publication, then please use our Emerald for Authors service information about how to choose which publication to write for and submission guidelines are available for all. Please visit www.emeraldinsight.com/authors for more information.

About Emerald www.emeraldinsight.com

Emerald is a global publisher linking research and practice to the benefit of society. The company manages a portfolio of more than 290 journals and over 2,350 books and book series volumes, as well as providing an extensive range of online products and additional customer resources and services.

Emerald is both COUNTER 4 and TRANSFER compliant. The organization is a partner of the Committee on Publication Ethics (COPE) and also works with Portico and the LOCKSS initiative for digital archive preservation.

*Related content and download information correct at time of download.

Downloaded by UNIVERSITY OF NOTTINGHAM At 18:57 21 January 2018 (PT)

Mechanical design and error prediction of a flexible manipulator system applied in nuclear fusion environment

Shanshuang Shi
Institute of Plasma Physics Chinese Academy of Sciences, Hefei, China and Laboratory of intelligent Machines, Lappeenrannan Teknillinen Yliopisto, Lappeenranta, Finland
Huapeng Wu
Laboratory of intelligent Machines, Lappeenrannan Teknillinen Yliopisto, Lappeenranta, Finland
Yuntao Song
Institute of Plasma Physics Chinese Academy of Sciences, Hefei, China, and
Heikki Handroos
Laboratory of intelligent Machines, Lappeenrannan Teknillinen Yliopisto, Lappeenranta, Finland

Downloaded by UNIVERSITY OF NOTTINGHAM At 18:57 21 January 2018 (PT)

Abstract

Purpose – The purpose of this paper is to introduce a development and error modeling of a serial redundant manipulator system applied in nuclear fusion environment. Detailed mechanical design of vacuum-compatible arms and actuators are presented, and manipulator flexibility is studied through experiments and model identification algorithm to evaluate the deformation.

Design/methodology/approach – First, the manipulator is designed to be several modular segments to obtain enough and flexible workspace inside the fusion device with narrow and complex geometries. Joint actuators with "rotation-linear-rotation" chains are developed to provide both huge reduction ratios and vacuum sealing. The redundant manipulator system has 11 degree of freedoms in total with a storage cask system to dock with the device vacuum vessel. In addition, to improve the position accuracy, an error prediction model is built based on the experimental study and back-propagation neural network (BPNN) algorithm.

Findings – Currently, the implementation of the manipulator system has been successfully carried out in both atmosphere and vacuum condition. Excellent performance indicates that the mechanical design is suitable. The validation of BPNN model shows an acceptable prediction accuracy (94∼98 per cent) compared with the real measurement.

Originality/value – This is a special robot system which is practically used in a nuclear fusion device in China. It will allow remote inspection and maintenance of plasma facing components in the vacuum vessel of fusion device without breaking the ultra-high vacuum condition during physical experiments. Its design, mechanism and error prediction strategy have great reference values to the similar robots in vacuum and temperature applications.

Keywords Robot design, Nuclear fusion, Flexible manipulator, Error prediction, BP neural network

Paper type Case study

Nomenclature

θ = pitch angle of the robot;
T_z = torque along z-axis;
T_x = torque along x-axis;
Fy = equivalent gravity;
Δx = errors of end clevis in x directions;
Δ_y = errors of end clevis in x directions;
$\Delta\theta_z$ = errors of end clevis along z-axis;
w_{ij} = weights between input and hidden layer;
θ_j = thresholds between input and hidden layer;
w_{jk} = weights between hidden and output layer;
θ_k = thresholds between hidden and output layer;
G_i = gravity load on link i;
m = mass of the link;
g = gravitational acceleration;
$CS\ (i)$ = local coordinate system of link i;
$\bar{r}_j^j$ = mass position vector of link j in CS (j);
T_i^j = transfer matrix from CS (i) to CS (j);
τ_{ij} = torgue on the Link i caused by Link j;
τ_i = total torque applied on the Link i;

1. Introduction

Experimental Advanced Superconducting Tokamak (EAST) is the world's first fully superconducting tokamak fusion device with non-circular cross-section which was built in China (Wan *et al.*, 2006). In recent years, with the increasing device

The current issue and full text archive of this journal is available on Emerald Insight at: **www.emeraldinsight.com/0143-991X.htm**

Industrial Robot: An International Journal
44/6 (2017) 711–719
© Emerald Publishing Limited [ISSN 0143-991X]
[DOI 10.1108/IR-04-2017-0066]

Received 27 December 2016
Revised 15 May 2017
Accepted 15 June 2017

Downloaded by UNIVERSITY OF NOTTINGHAM At 18:57 21 January 2018 (PT)

performance and experimental parameters, EAST tokamak has made a series of important research results and scientific discoveries (Li *et al.*, 2013; Wang *et al.*, 2014). However, EAST inner components will also be facing increasingly tough operating environment with huge heat flux as the plasma current during discharges becoming higher and higher. It leads the plasma facing components (PFCs) easily to be damaged, in which case the effective running time cannot be guaranteed (Yang *et al.*, 2016; Li *et al.*, 2016). Therefore, it is essential for the timely maintenance based on the condition of damaged internal components in the experimental period. For the purpose of real-time detection and rapid repairing of the damaged internal components during plasma discharges, EAST-articulated maintenance arm (EAMA) system has been developed since 2013. It will allow remote inspection and simple repair of PFCs in EAST vacuum vessel (VV) without breaking down the ultra-high vacuum condition ($\sim 10^{-5}$Pa).

The articulated inspection arm (AIA) robot is a related application which was specially developed for International Thermonuclear Experimental Reactor (ITER) fusion reactor (Shimomura *et al.*, 1999) and demonstrated in Tore-supra tokamak device (Gargiulo *et al.*, 2009). It is able to inspect the in-vessel components under 120°C and 10^{-6} Pa condition with a 200 mm maximum position error due to the flexibility of the 10-meter cantilever structure (Perrot *et al.*, 2012). The poor position accuracy means that the robot can only run in the middle of the VV rather than operate at close-range or even touch the tokamak wall from a security point of view. Similar to the AIA robot, the effect of gravity will also cause huge flexible deformation on EAMA, which is unacceptable for running inside a narrow and complex-shaped space as EAST VV. Figure 1 shows the cantilever structure of fully assembled EAMA robot without end-effector and the finite element simulation results for the position error.

Elastic deformations due to gravity will cause robot trajectory planning to be quite a complicated issue, especially for serial long-reach manipulators. Error prediction strategy should always be studied in advance if high accuracy is required. In fact, research on robotic flexibility has become a matter of great concern in recent years because of the pursuit of high accuracy and reliability. Especially for cable-driven manipulators, error modeling is essential for final control performance (Chen *et al.*, 2011; Zi *et al.*, 2014a, 2014b). Normally, two methods could be considered to build the flexible model for error predicting. On one hand, the mathematic model of flexible multibody dynamics can be derived from classical mechanical theories such as the Newton–Euler formulation, the Lagrange formulation, etc. Then either the finite element method or the assumed modes method can be used to truncate the dynamic formulations for rapid solution with an appropriate accuracy (Dwivedy and Eberhard, 2006). On the other hand, for some complex systems with several uncertain coupling factors, the flexible model can be identified using some computing algorithms without considering the complicated mechanical model and highly nonlinear formulations. For example, a genetic algorithm is used to optimize dynamical performance of a cable parallel manipulators (Zi *et al.*, 2014a, 2014b). Other examples, based on fuzzy algorithm (Schiavo and Luciano, 2001) and artificial neural network approach (Liu, 2012), can also be found in similar applications of flexible robots.

Figure 1 Cantilever structure of EAMA robot

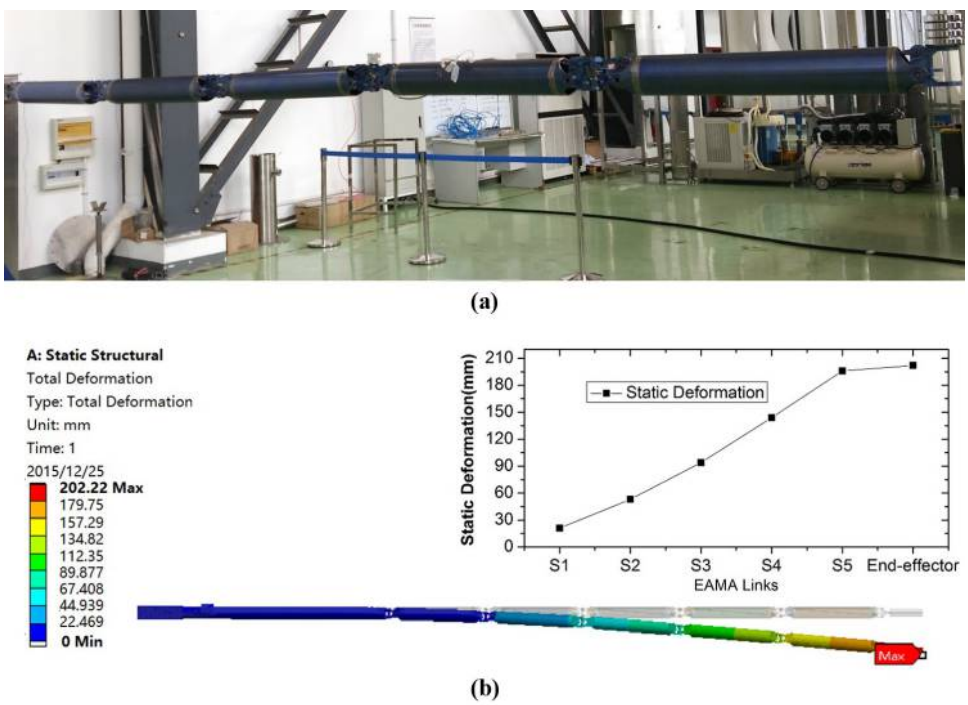

Notes: (a) The fully assembled EAMA robot without end-effector; (b) the finite element simulation results for the position errors of different links

Industrial Robot: An International Journal
Volume 44 · Number 6 · 2017 · 711–719

Downloaded by UNIVERSITY OF NOTTINGHAM At 18:57 21 January 2018 (PT)

For the case study of EAMA manipulator, the mathematical modeling using classical mechanics theories is difficult to obtain high accuracy and efficiency owing to two reasons. First, the complicated mechanism, transmission chain and multi links make the accurately flexible modeling to be quite a difficult issue. Second, the dynamic formulations with high nonlinearity is not necessary as the manipulator speed is extremely low (less than 0.5 degree per second), which means that the dynamic behaviors are slight enough compared with the gravity effect. Therefore, static modeling can be a better choice for error predicting with a relatively high accuracy.

In this paper, the conceptual design of the manipulator system is first introduced. An experimental study was deployed to measure the errors of EAMA prototype assembled with different loads through a load-deflection platform. Based on the experimental data, a static error prediction model was built and trained by using back-propagation neural network (BPNN) algorithm. The results show an acceptable prediction accuracy while around 5 per cent predicting error compared with the real measurement. Furthermore, the mathematic formulation for static loads of robot joints in arbitrary position was derived. The calculated joint loads can be treated as the input of the trained BPNN model to predict the robot errors in arbitrary positions and postures without any experiments and measurements in future.

2. Manipulator system design

2.1 Overall introduction

EAMA system consists of a highly redundant manipulator, one mobile base, five serial arms and an end-effector (CCD cameras, gripper, etc.) for dedicated functional operations. Besides, a storage cask facility was developed to maintain the equivalent vacuum environment for the manipulator before docking with EAST VV. Figure 2 shows an overall schematic view of EAMA system and the robot specifications is given in Table I (Shi *et al.*, 2016).

2.2 Modular arm design

For the manipulator arms, an identical modular design with a parallelogram mechanism was adopted for all five arm segments. Each segment can provide both rotation and elevation motions by integrating yaw and pitch actuator inside one modular arm segment. As shown in Figure 3, the parallelogram structure is composed of two clevis (yaw joints), horizontal rods, an arm tube and a diagonal rod (pitch actuator). The five-bar mechanism can produce a huge reduction ratio and withstand strong torques generated from the cantilever arms and gravity effects. In addition, the axis of the yaw joint will always be kept in a vertical direction owing to the motion characteristics of the parallelogram structure.

Forward kinematics model of the entire manipulator was established based on the EAMA configuration diagram shown in Figure 4. Finally, the available workspace can be calculated by Monte Carlo method (Doucet *et al.*, 2001) after excluding collisions, as shown in Figure 5. The cloud of workspace presents that the EAMA robot can reach almost everywhere in the EAST VV except for the area close to the entrance because of the length limits. The percentage of available space can reach to more than 90per cent.

Table I Specifications of EAMA manipulator

Vacuum	10^{-5} Pa to 1 atm
Temperature	Running:80°C; baking:120°C
Workspace	In-vessel: R = 1920, a = 550 mm
DOFs	1(base) + 7(arm) + 3(end-effector)
Payload	25 kg
Dimension	Radius: 160 mm, length: 8.8 m
Weight	<100 kg (arm)
Required accuracy	±20 mm
Function	Inspection and simple repair

Figure 2 Layout of EAMA system

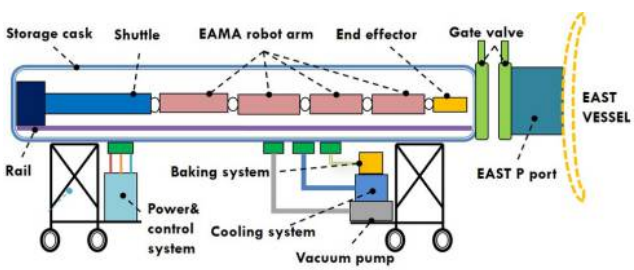

Figure 3 Modular design of EAMA robot arms

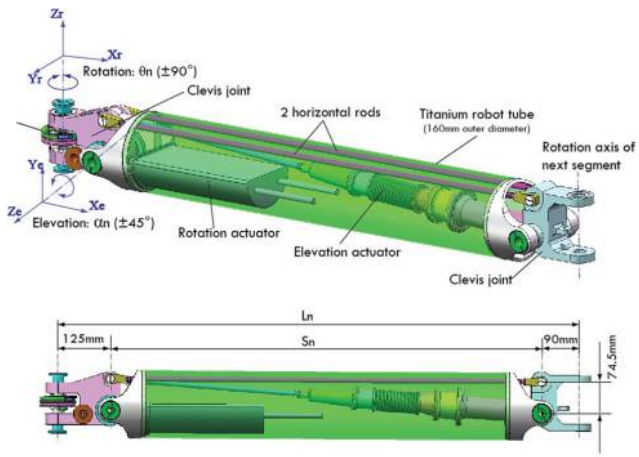

Note: Five segments with identical principle design, the first to third segments have only rotation motions by using rigid rods instead of elevation actuators; the forth and fifth segments have both rotation and elevation motions

Figure 4 Kinematic model of EAMA manipulator

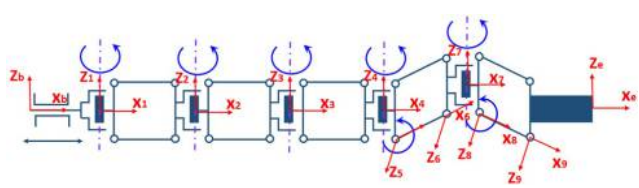

Downloaded by UNIVERSITY OF NOTTINGHAM At 18:57 21 January 2018 (PT)

Figure 5 Available workspace in EAST VV

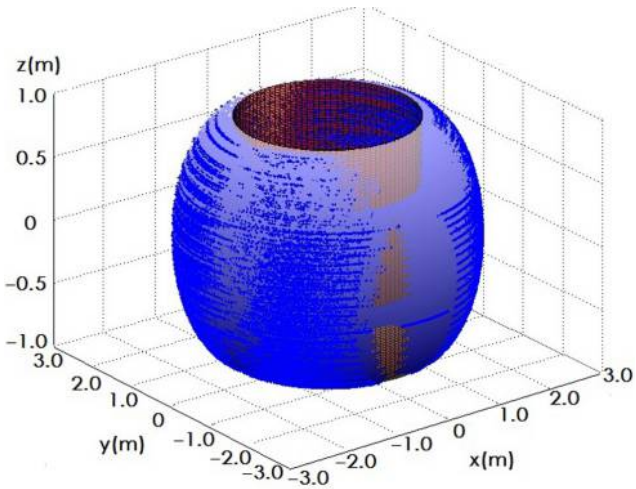

2.3 Vacuum-compatible actuators

Motion actuators are placed inside robot tubes. The rotation actuator is connected to the tube, while the elevation actuator is located diagonally in the parallelogram. To avoid polluting the ultra-high vacuum condition inside the EAST VV, motion actuators with dynamic sealing have been developed. All the high-speed components (motors, gears, etc.) which should be lubricated very well, are sealed in boxes by welding bellows so that high temperature grease can be used. Meanwhile, some low-speed components (joint bearings and bushes) use MoS2-Ti-C coating films for solid lubricating. The detailed design of the motion actuators can be summarized as follows:

2.3.1 Yaw actuator

As shown in Figure 6, first two planetary roller screws transfer the rotation motion produced by high-temperature motor and reducers into two parallel linear motions. The two screws connected with two steel cables move at a same speed but in opposite directions to transmit the linear motions to the yaw joint through bellows welded together with the seal box. The cables are assembled with a pulley system attached to the yaw joint to produce the rotation motion. The whole transmission process can be summarized as a "rotation-linear-rotation" chain. Two benefits are provided by this chain: dynamic sealing to protect the vacuum condition and a huge reduction ratio to generate enough driving torque (1:30820 from motor to yaw joint).

2.3.2 Pitch actuator

As shown in Figure 7, the pitch actuator has a similar "rotation-linear-rotation" chain as the yaw actuator. The difference is that only one roller screw is used here to

Figure 6 Pulley system layout and detailed design of EAMA yaw actuator

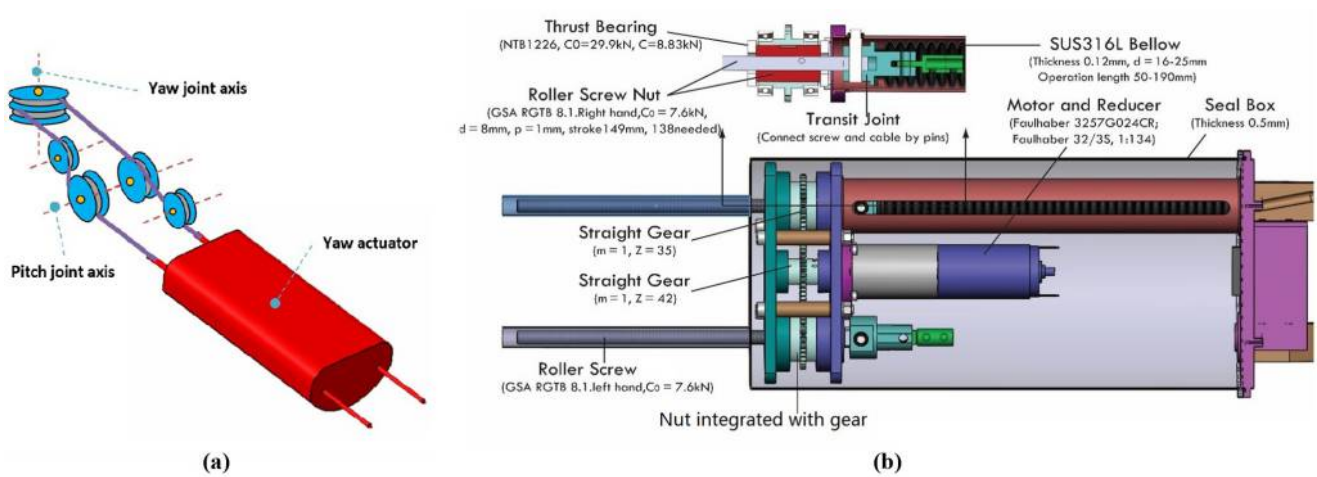

Notes: (a) Pulley system of the yaw joint; (b) section view and detailed design of the yaw actuator

Figure 7 Detailed design of EAMA pitch actuator

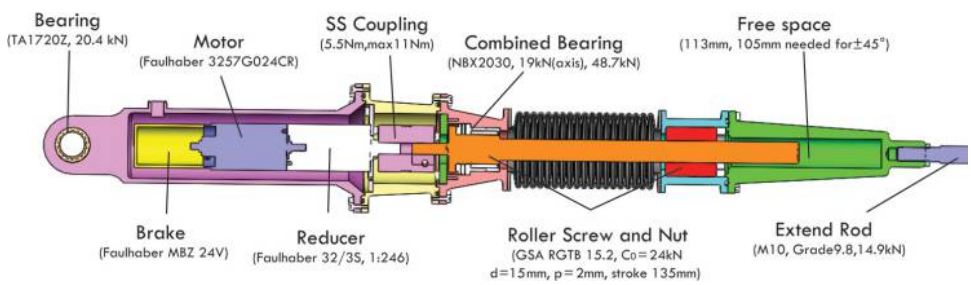

transfer the rotation to a linear motion. As the pitch actuator is located in the diagonal position, the changes in diagonal length will lead the whole parallelogram structure to be elevated, while other link length are fixed articulately. The reduction ratio can reach up to 1:51660.

Currently, all of the manipulator components have been developed. The prototype of the EAMA modular arm and actuators are given in Figure 8.

3. Experimental study

Compared with an industrial robot, the EAMA system has more significant position errors which are caused by the flexibilities of long-reach links as well as the complicated joints and transmission chains. An accurate theoretical model for error prediction is difficult to build as there are multiple time-varying factors (and relative weightings) that affect system stiffness. Therefore, a load-deflection platform was considered for the experimental study of the manipulator flexible properties. Figure 9 illustrates the platform design. Three types of external loads (mass in the y direction, torques along the *x*- and *z*-axes) as the system inputs were applied to the prototype of the EAMA modular arm. Different payloads were attached to two adjustable beams in the x and z directions to generate different torques on the robot joint. Correspondingly, three items of position errors (deflections in the x and y directions, angles along the *z*-axis) were measured by a laser tracker. Finally, 272 sets of load-deflection data under different loads were recorded, which were treated as the samples to train the BPNN prediction model.

Figure 9 The illustration and implementation of load-deflection platform

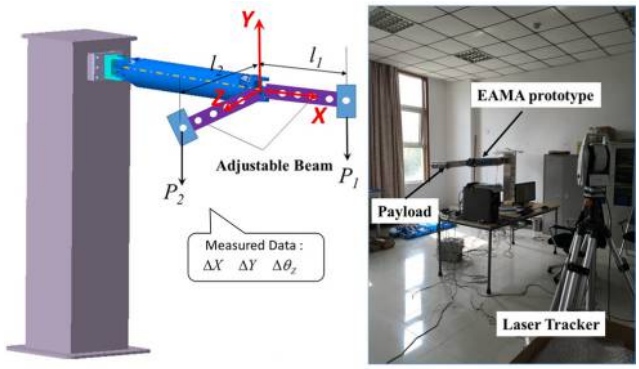

Note: Different payloads were attached to two adjustable beams in *x* and *z* direction to generate different torques on robot joint

4. Back-propagation neural network prediction model

In a BPNN algorithm, several strongly coupled neurons are used to approximate the nonlinear functions. The learning process can be summarized as two steps (Negnevitsky, 2005). First, a set of training data is input to the multi-layer network to obtain relevant output. Two kinds of functions will be used: a linear transfer function with different weights and thresholds [equation (1)] and a sigmoid activation function [equation (2)]. Second, an error is calculated by

Figure 8 Prototype of the EAMA modular arm and actuators

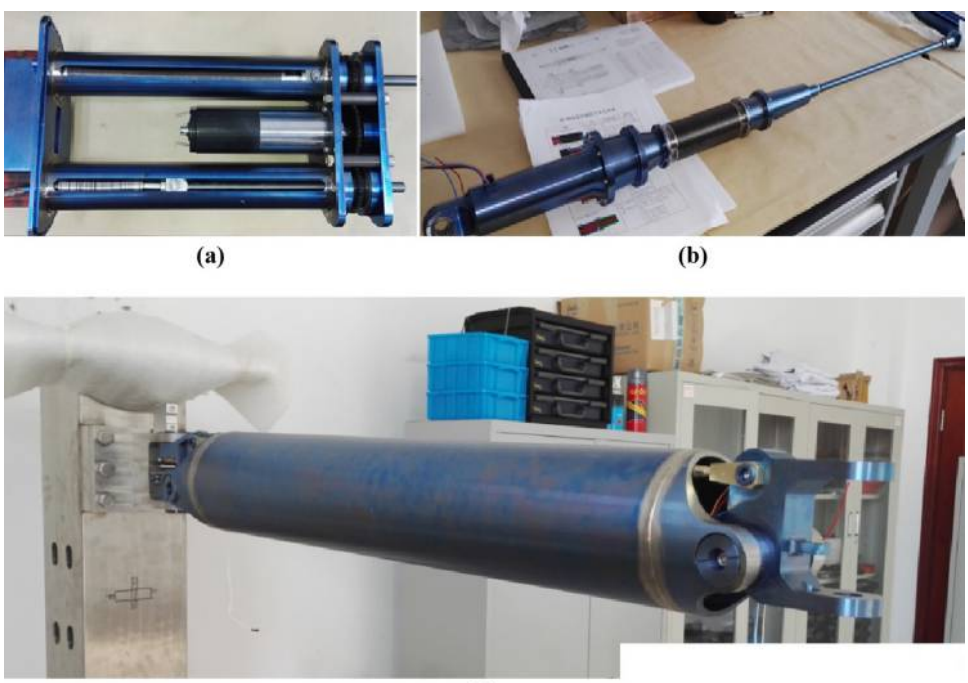

Notes: (a) Yaw actuator; (b) pitch actuator; (c) modular arm prototype

Downloaded by UNIVERSITY OF NOTTINGHAM At 18:57 21 January 2018 (PT)

comparing the output with its expected value. Normally, the expected values are obtained from experimental measurements. Then the error is propagated backwards through the network to modify the weights and thresholds of the coupled neurons. The rule for modifying weights and thresholds should always aim at reducing the error.

$$X = \sum_{i=1}^{n} x_i w_i - \theta \tag{1}$$

$$Y^{sigmoid} = \frac{1}{1 + e^{-X}} \tag{2}$$

For error prediction of EAMA manipulator, a final three-layer network has been built as the topological structure shown in Figure 10:

- Four neurons in input layer: θ – the pitch angle of robot, T_z – the torque along z-axis, T_x – the torque along x-axis, F_y – the equivalent gravity;
- single hidden layer with eight neurons;
- Three neurons in output layer: the errors of end clevis in different directions: Δx, Δy and $\Delta\theta_z$;
- w_{ij} and θ_j denote the weights and thresholds between input and hidden layer; v_{jk} and θ_k denote the weights and thresholds between hidden and output layer.

Figure 10 The topological structure of BPNN model

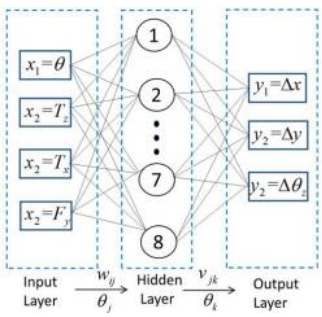

The 272 sets of sample data were divided into two parts:

1. 243 sets of data were utilized for network training, among which 70 per cent for training, 15 per cent for testing and 15 per cent for validation; and
2. 29 extra measurement data were used to check the prediction accuracy of the BPNN model after training.

The mathematical model was established by the Neural Network toolbox in MATLAB 2015a environment. The network training function is *Traingdx*, which is able to automatically adjust learning rate and convergence rate based on the classical BP algorithm (Shi *et al.*, 2009). The optimized values of the learning and convergence rate were set to be respectively 0.02 and 1e-6 after comparing the performance of different couples of parameters. The training was ended at epoch 6,751, while the mean squared error was converged to 6.7717e-7 (Figure 11).

To evaluate the prediction performance of the trained BPNN model, the extra 29 sets of load data were calculated by the offline BPNN model with the trained weights and thresholds listed in Tables II and III. Figure 12 gives the fitting situation between predicted and measured values which indicate a prediction error range from 2 to 6 per cent (Figure 13). Considering the huge flexibility and complicated structure of EAMA manipulator, the predicting accuracy is acceptable. The trained BPNN model can be integrated into the control system to compensate the deflection error and improve the final position accuracy.

Figure 11 The training process of BPNN model

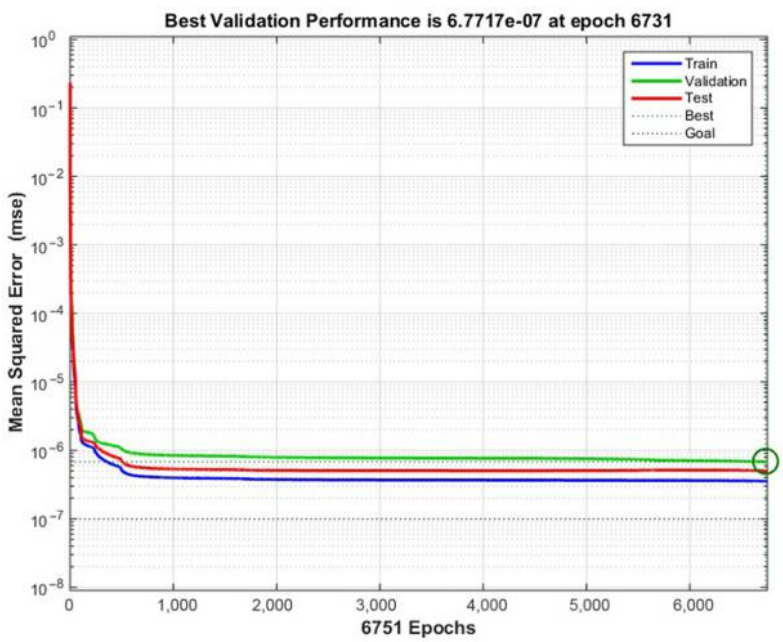

Downloaded by UNIVERSITY OF NOTTINGHAM At 18:57 21 January 2018 (PT)

Downloaded by UNIVERSITY OF NOTTINGHAM At 18:57 21 January 2018 (PT)

Table II The trained weights and thresholds between input and hidden layer

j	w_{ij} (i = 4, j = 8)				θ_j
1	−0.22532639	−0.021457862	0.000143862	0.021266973	1.168193494
2	−0.36576382	0.002737846	0.000151412	0.061871295	0.506266839
3	0.374547274	0.02131777	−0.000453784	−0.022556882	0.265934803
4	−0.324228676	0.000747825	0.000236239	0.016785358	0.113202306
5	−0.313983181	−0.00378339	0.000254887	0.005711087	−0.02688637
6	−1.88891379	−0.004668008	−0.0000337	−4.908188396	−2.751156441
7	0.389308685	−0.011864381	−0.000147494	0.045723211	0.828719931
8	0.33108	−0.0137	−0.00012	0.036749	0.816560631

Table III The trained weights and thresholds between hidden and output layer

k	v_{jk} (j = 8, k = 3)								θ_k
1	46.3462	−19.279	−17.9038	54.933	−81.8616	−0.01364	89.21414	−121.38	−11.933
2	7.83777	−30.161	−15.0365	181.49	−183.839	−0.05781	−73.7377	71.93208	−12.3189
3	−23.872	9.81833	−19.0517	30.596	−69.5353	0.016233	106.448	−146.954	41.26604

Figure 12 The fitting situation between predicted and measured values

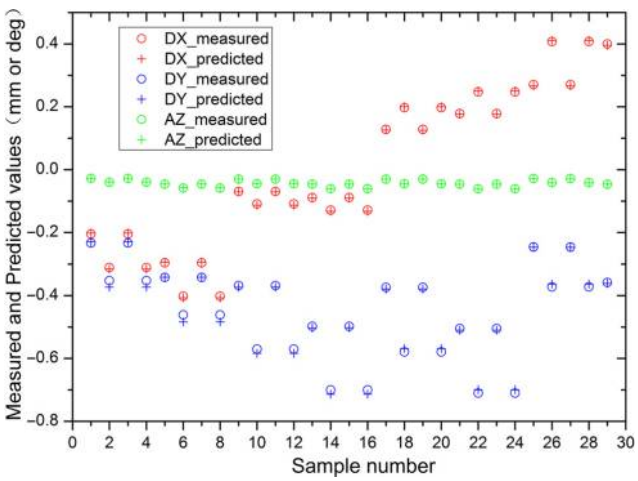

Figure 13 The prediction error of the trained BPNN model

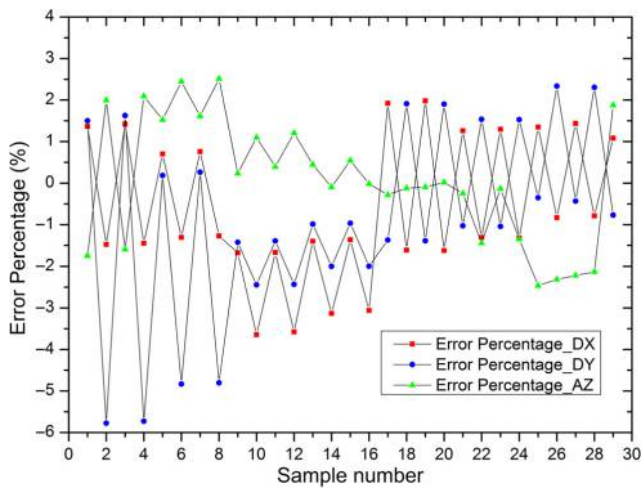

5. Formulation of static loads

As the motion speed of EAMA manipulator is quite slow (less than 0.6 deg/s), dynamics are not significant when considering the payloads on each joint. To simplify the calculation, static loads due to gravity were derived using the model built in Figure 14. With the load results, the deflections of all segments can be predicted with the trained BPNN model in former section.

Considering the static loads on the end point O_i of Link i, first, the gravity load can be easily written as equation (3):

$$G_i = \sum_{j=i}^{n} m_j g \tag{3}$$

For the torques, the effect on Link i caused by Link j was first considered as equation (4), among which the torque was divided into two parts that, respectively, represent the torque along x (τ_{ij}^{x}) and y axis (τ_{ij}^{y}) in the local coordinate system of

Figure 14 Modeling of static loads

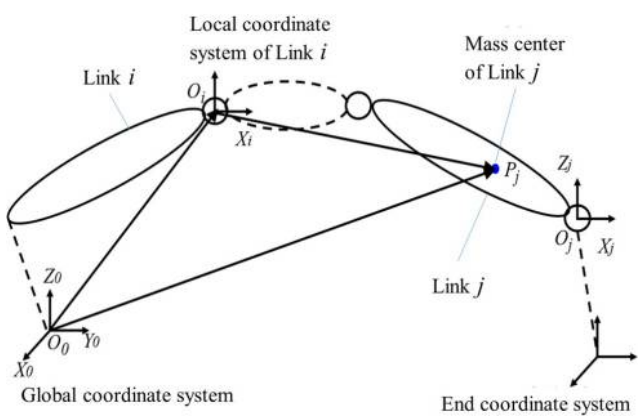

Downloaded by UNIVERSITY OF NOTTINGHAM At 18:57 21 January 2018 (PT)

Link i-CS (i). Besides, $\overrightarrow{O_iP_j}^{(i)}$ is the position vector of point P_j (mass center of Link j) with respect to point O_i in CS (i), while $g_y = [0 \quad g \quad 0 \quad 0]$ and $g_x = [g \quad 0 \quad 0 \quad 0]$:

$$\tau_{ij} = \begin{bmatrix} \tau_{ij}^x \\ \tau_{ij}^y \end{bmatrix} = \begin{bmatrix} m_j g_y \cdot \overrightarrow{O_iP_j}^{(i)} \\ m_j g_x \cdot \overrightarrow{O_iP_j}^{(i)} \end{bmatrix} \tag{4}$$

Furthermore, $\overrightarrow{O_iP_j}^{(i)}$ can be derived into equation (5), where T_i^j is the transfer matrix from CS (i) to CS (j) which can be obtained using D-H method (Denavit and Hartenberg, 1955). $\bar{r}_j^j$ is the position vector of mass center P_j in CS (j), which is determined by the geometry and mass properties of Link j:

$$\overrightarrow{O_iP_j}^{(i)} = T_i^j \bar{r}_j^j \tag{5}$$

Combining equation (4) and equation (5), the total torque applied on the end point O_i of Link i can be derived as:

$$\tau_i = \begin{bmatrix} \tau_i^x \\ \tau_i^y \end{bmatrix} = \begin{bmatrix} \sum_{j=i}^{n} \left(m_j g_x \cdot T_i^j \bar{r}_j^j \right) \\ \sum_{j=i}^{n} \left(m_j g_x \cdot T_i^j \bar{r}_j^j \right) \end{bmatrix} \tag{6}$$

With the formulations above, the static loads on each joint can be calculated when the manipulator position is known. The loads can be treated as the input of the trained BPNN model for error evaluation without any experiments and measurements in future.

6. Conclusions

An articulated manipulator system applied in fusion environment has been developed in China for the purpose of real-time detection and rapid repairing of the damaged internal components in EAST tokamak device. The mechanical design of EAMA system was introduced first in this paper, including the modular parallelogram mechanism, the "rotation-linear-rotation" actuator design for dynamic sealing, etc. The operation activities of EAMA robot were successfully implemented in EAST under high vacuum and temperature conditioning as shown in Figure 15. Excellent performance owes to two superiorities of the mechanical design:

1. huge reduction ratio (more than 50000:1) ensure a micro motor (Φ32 mm) driving torque of more than 1,000 Nm, which makes the mechanism more integrated and load-bearing; and
2. the vacuum-compatible actuators ensure grease lubrication for high-speed components without polluting the high vacuum condition.

In addition, to predict and compensate the flexible errors due to gravity effect, a load-deflection platform directed to EAMA prototype was built. Excellent performance indicates that the mechanical design is suitable. After training, the fitting situation between BPNN predicted and experimental measured values indicate a prediction error range from 2 to 6 per cent. Finally, the static loads of each manipulator link was formulated, which can be integrated with the BPNN model for the error evaluation in control system. The experiments in EAST 1:1 scale mockup facility shown around ±15~20 mm of accuracy after compensating (Figure 16). The error was more than 100 mm without any compensation. Some visual stereoscopic positioning method could be considered if higher accuracy was needed in the future work. The conceptual design and error prediction strategy introduced in the paper can give beneficial reference to the similar robotic applications in vacuum and temperature condition.

Figure 15 Commissioning of the EAMA manipulator system in EAST VV

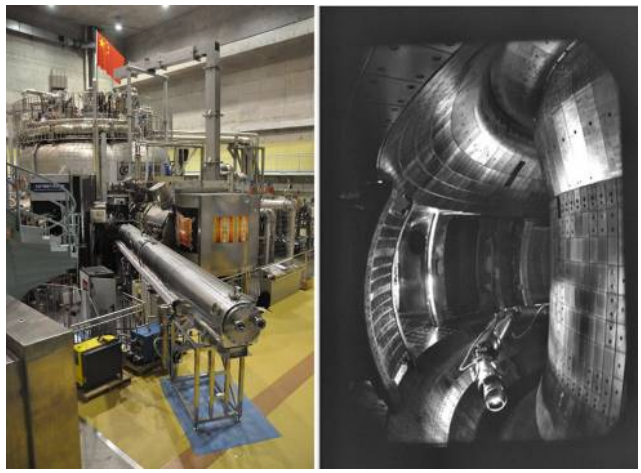

Figure 16. Accuracy test carried out in the EAST 1:1 scale mockup facility

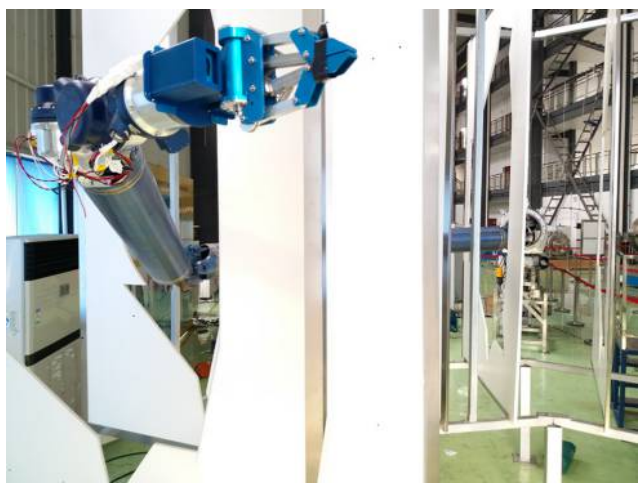

References

Chen, Q., Chen, W., Liu, R. and Zhang, J. (2011), "Error analysis and flexibility compensation of a cable-driven humanoid-arm manipulator", *IEEE International Conference on Robotics and Automation*, Vol. 19 No. 6, pp. 988-993.

Denavit, J. and Hartenberg, R.S. (1955), "A kinematic notation for lower-pair mechanisms based on matrices", *Journal of Applied Mechanics*, Vol. 22, pp. 215-221.

Doucet, A., Freitas, N.D. and Gordon, N. (2001), "An introduction to sequential Monte Carlo methods", *Sequential Monte Carlo Methods in Practice*, Springer, New York, NY.

Dwivedy, S.K. and Eberhard, P. (2006), "Dynamic analysis of flexible manipulators, a literature review", *Mechanism and Machine Theory*, Vol. 41 No. 7, pp. 749-777.

Gargiulo, L., Bayetti, P., Bruno, V., Hatchressian, J.C., Hernandez, C., Houry, M., Keller, D., Martins, J.P., Measson, Y., Perrot, Y. and Samaille, F. (2009), "Operation of an ITER relevant inspection robot on ToreSupra tokamak", *Fusion Engineering and Design*, Vol. 84 No. 2, pp. 220-223.

Li, W.X., Song, Y.T., Ye, M.Y., Peng, X.B., Wu, S.T., Qian, X.Y. and Zhu, C.C. (2016), "Thermo-mechanical and damage analyses of EAST carbon divertor under type-I ELMy H-mode operation", *Fusion Engineering and Design*, Vol. 105, pp. 15-21.

Li, J., Guo, H.Y., Wan, B.N., Gong, X.Z., Liang, Y.F., Xu, G. S., Gan, K.F., Hu, J.S., Wang, H.Q., Wang, L., Zeng, L., Zhao, Y.P., Denner, P., Jackson, G.L., Loarte, A., Maingi, R., Menard, J.E., Rack, M. and Zeng, L. (2013), "A long-pulse high-confinement plasma regime in the experimental advanced superconducting tokamak", *Nature Physics*, Vol. 8 No. 3, pp. 817-821.

Liu, G.P. (2012), *Nonlinear Identification and Control: A Neural Network Approach*, Springer Science & Business Media, New York, NY.

Negnevitsky, M. (2005), *Artificial Intelligence: A Guide to Intelligent Systems*, Pearson Education, London.

Perrot, Y., Gargiulo, L., Houry, M., Kammerer, N., Keller, D., Measson, Y., Piolain, G. and Verney, A. (2012), "Long-reach articulated robots for inspection and mini-invasive interventions in hazardous environments: Recent robotics research, qualification testing, and tool developments", *Journal of Field Robotics*, Vol. 29 No. 1, pp. 175-185.

Schiavo, A.L. and Luciano, A.M. (2001), "Powerful and flexible fuzzy algorithm for nonlinear dynamic system identification", *IEEE Transactions on Fuzzy Systems*, Vol. 9 No. 6, pp. 828-835.

Shi, S., Song, Y., Cheng, Y., Villedieu, E., Bruno, V., Feng, H., Wo, H., Wang, P., Hao, Z., Li, Y. and Wang, K. (2016), "Conceptual design main progress of EAST articulated maintenance arm (EAMA) system", *Fusion Engineering and Design*, Vol. 104, pp. 40-45.

Shi, Y., Zhao, X.T., Zhang, Y.M. and Ren, N.Q. (2009), "Back propagation neural network (BPNN) prediction model and control strategies of methanogen phase reactor treating traditional chinese medicine wastewater (TCMW)", *Journal of Biotechnology*, Vol. 144 No. 1, pp. 70-74.

Shimomura, Y., Aymar, R., Chuyanov, V., Huguet, M. and Parker, R. (1999), "ITER overview", *Nuclear Fusion*, Vol. 39 No. 9Y, pp. 1295.

Wan, Y., Li, J. and Weng, P. (2006), "First engineering commissioning of EAST tokamak", *Plasma Science and Technology*, Vol. 8 No. 3.

Wang, H.Q., Xu, G.S., Wan, B.N., Ding, S.Y., Guo, H.Y., Shao, L.M., Liu, S.C., Xu, X.Q., Wang, E., Yan, N. and Naulin, V. (2014), "New edge coherent mode providing continuous transport in long-pulse h-mode plasmas", *Physical Review Letters*, Vol. 112 No. 18, p. -185004.

Yang, Z., Fang, J., Gong, X., Gan, K., Luo, J., Zhao, H. and Chen, M. (2016), "The study of heat flux for disruption on experimental advanced superconducting tokamak", *Physics of Plasmas (1994-Present)*, Vol. 5 No. 23, p. 052502.

Zi, B., Ding, H., Wu, X. and Kecskeméthy, A. (2014a), "Error modeling and sensitivity analysis of a hybrid-driven based cable parallel manipulator", *Precision Engineering*, Vol. 38 No. 1, pp. 197-211.

Zi, B., Ding, H., Cao, J., Zhu, Z. and Kecskeméthy, A. (2014b), "Integrated mechanism design and control for completely restrained hybrid-driven based cable parallel manipulators", *Journal of Intelligent & Robotic Systems*, Vol. 74 No. 3, pp. 643-661.

Corresponding author

Shanshuang Shi can be contacted at: shiss@ipp.ac.cn

Downloaded by UNIVERSITY OF NOTTINGHAM At 18:57 21 January 2018 (PT)

For instructions on how to order reprints of this article, please visit our website:
www.emeraldgrouppublishing.com/licensing/reprints.htm
Or contact us for further details: **permissions@emeraldinsight.com**